J. Membrane Biol. 201, 97–107 (2004)
DOI: 10.1007/s00232-004-0711-x

The Journal of
Membrane
Biology

Importance of Conserved Acidic Residues in MntH, the Nramp homolog of *Escherichia coli*

H.A.H. Haemig, R.J. Brooker
Department of Genetics, Cell Biology and Development, and the Biotechnology Institute, University of Minnesota, Minneapolis, MN 55455, USA

Received: 26 May 2004/Revised: 4 August 2004

Abstract. A bioinformatic approach was used for the identification of residues that are conserved within the Nramp family of metal transporters. Site-directed mutagenesis was then carried out to change six conserved acidic residues (i.e., Asp-34, Glu-102, Asp-109, Glu-112, Glu-154, and Asp-238) in the *E. coli* Nramp homolog *mntH*. Of these six, five of them, Asp-34, Glu-102, Asp-109, Glu-112, and Asp-238 appear to be important for function since conservative substitutions at these sites result in a substantial loss of transport function. In addition, all of the residues within the signature sequence of the Nramp family, DPGN, were also mutated in this study. Each residue was changed to several different side chains, and of ten site-directed mutations made in this motif, only P35G showed any measurable level of $^{54}Mn^{2+}$ uptake with a V_{max} value of approximately 10% of wild-type and a slightly elevated K_m value. Overall, the data are consistent with a model where helix breakers in the conserved DPGN motif in TMS-1 provide a binding pocket in which Asp-34, Asn-37, Asp-109, Glu-112 (and possibly other residues) are involved in the coordination of Mn^{2+}. Other residues such as Glu-102 and Asp238 may play a role in the release of Mn^{2+} to the cytoplasm or may be involved in maintaining secondary structure.

Key words: Symporter — Nramp — Manganese transport

Introduction

Iron and manganese are essential metals that are necessary as redox-active cofactors for a variety of enzymes and protein complexes including cytochromes, oxygen-binding proteins, free-radical detoxifying enzymes, and the photosynthetic water-oxidizing complex, to mention a few (Crowley, Traynor & Weatherburn, 2000). The ability to readily accept and donate electrons makes Fe^{2+}/Fe^{3+} and Mn^{2+}/Mn^{3+} critical components for a variety of biochemical reactions. Unfortunately, this same chemistry accounts for the potential toxicity of certain transition metals. For example, free iron catalyzes the Fenton reaction in which H_2O_2 is converted to the OH free radical. Such free radicals may attack proteins and DNA thereby causing cellular damage. For this reason, nearly all of the iron in cells, as well as all extracellular iron in multicellular organisms, is tightly bound to proteins, or within iron-sequestering complexes such as ferritin (Andrews, Robinson & Rodriguez-Quinones, 2003).

Among prokaryotes, fungi, plants, and animals, metal ions such as iron and manganese are transported into cells by a wide variety of mechanisms. In the case of iron, some of these transporters recognize the chelated form of the metal. For example, many species of bacteria secrete siderophores that chelate iron, which is then transported into the cell via a specific siderophore-mediated uptake system (*see* Braun & Braun, 2002; Winkelmann, 2002; Andrews et al., 2003 for recent reviews). Alternatively, some transporters recognize the free form of iron or manganese. These proteins typically transport the reduced form (i.e., Fe^{2+} and Mn^{2+}) of the metal. Within the last decade, such transporters have been found to play a key role in the uptake of dietary iron in mammals and fungi, and in the uptake of manganese in prokaryotes. In particular, the natural resistance-associated macrophage (Nramp) family was discovered to couple the transport of divalent metal cations with hydrogen ions (Fleming et al., 1997; Gunshin et al., 1997). Nramp1 and Nramp2 were first identified in mice, and it was predicted that both were membrane proteins because of the presence of a highly

Correspondence to: R.J. Brooker; email: robert-b@biosci.cbs.umn.edu

conserved hydrophobic core and helical periodicity of sequence conservation (Gruenheid et al., 1995). Nramp2 was determined to have broad substrate specificity (Fe^{2+}, Mn^{2+}, Co^{2+}, Cu^{2+}, Ni^{2+}, Pb^{2+}, and Zn^{2+}) and transport is proton-coupled (Gunshin et al., 1997).

With the burgeoning number of genome sequences that have become available in recent years, sequence alignments have revealed a high level of sequence conservation among Nramp homologs from a wide variety of different species. For example, at the amino-acid level, mammalian Nramp homologs exhibit sequence conservation with *E. coli* (39%), *Saccharomyces cerevisiae* (41%), *Arabidopsis thaliana* (60%), *Caenorhabditis elegans* (67%), and *Drosophila melanogaster* (70%) (Pinner et al., 1997). Several complementation studies between Nramps of different species have demonstrated that within the Nramp family, structural similarity is paralleled by functional conservation (Pinner et al., 1997; D'Souza et al., 1999; Curie et al., 2000; Thomine et al., 2000).

Recently, the bacterial Nramp homologs from *E. coli* and *Salmonella typhimurium* have been characterized and shown to have a broad specificity, recognizing several transition metals, but with a noticeably higher affinity for divalent manganese (Kehres et al., 2000; Makui et al., 2000). The Nramp homolog in these two bacterial species has been named *mntH*, since its physiological role is postulated to be the uptake of manganese rather than iron (Kehres et al., 2000; Makui et al., 2000).

Recent phylogenetic studies identified 3 groups of bacterial Nramp homologs (A, B, and C) with A and B bearing the most resemblance to each other and group C being more similar to eukaryotic Nramp genes (Cellier et al., 2001; Richer et al., 2003). Expression of group B and C genes in *E. coli* (which belongs to group A) showed conservation of divalent metal ion uptake (Richer et al., 2003). Group A and group B genes may have been transferred to the eukaryotic genome by mitochondria, which then evolved into the eukaryotic Nramp group. By comparison, it has been speculated that members of group C have a higher likelihood than A or B to have been living in close contact with primitive eukaryotic cells from which they acquired an intronless prototype Nramp gene (Richer et al., 2003). Capture of an Nramp-derived protein by an opportunistic bacterium could be advantageous in resisting host Nramp-mediated defenses.

Though members of the Nramp family play a key role in the dietary uptake of iron in mammals, plants, and fungi, and in the uptake of manganese in bacteria, little is known regarding their structure/function relationships. Naturally occurring mutations in mice and rats (G185R) are known to inhibit function and thereby lead to defects in the dietary absorption of iron and the ability to resist infection by various bacterial pathogens (Fleming et al., 1997; Su et al., 1998). More recently, a mutagenesis study of mouse Nramp2 suggested that three negatively charged residues are essential for transport, and two histidine residues may play a role in the pH regulation of transport activity (Lam-Yuk-Tseung et al., 2003). Another mutagenesis study highlighted the potential importance for metal binding and specificity of several residues within the first predicted extracellular loop of rat Nramp2 (Cohen, Nevo & Nelson, 2003). In addition, attempts to understand structure/function relationships have involved the approach of site-directed spin labeling in *Mycobacterium* Nramp (Reeve et al., 2002).

Due to the high degree of sequence conservation among Nramp homologs and the ease of working with bacteria, we have chosen the bacterial homolog (*mntH*) from *E. coli* to investigate structure/function relationships and the potential importance of the conserved acidic residues in the Nramp family. In the current study, we have systematically altered six conserved acidic residues (D34, E102, D109, E112, E154, and D238). The results indicate that five of these residues are important for function. Two of them, D34 and E102, which are predicted to be on transmembrane segments, appear to be essential for transport function since conservative substitutions result in a complete loss of activity.

Materials and Methods

Reagents

$MnCl_2$ and MES (2-N-morpholino ethane sulfonic acid) were purchased from Sigma (St. Louis, MO). ^{54}Mn was purchased from Perkin Elmer (Boston, MA). Restriction enzymes and DNA ligase were purchased from New England Biolabs (Beverly, MA). The QuikChange kit was purchased from Stratagene (La Jolla, CA). All remaining reagents were of analytical grade.

Bacterial Strains and Methods

The relevant genotypes of the bacterial strains and mutant plasmids are described in Table 1. Plasmid DNA was purified using the Eppendorf Plasmid Mini DNA Kit (Westbury, NY). Restriction digests and ligations were performed according to the manufacturers' recommendations. Cell cultures were grown in YT media (Kraft et al., 1998) supplemented with chloramphenicol (30 μg/mL).

Plasmid Constructions

The plasmid, pSU2718, was constructed using methods described by Martinez and colleagues (Martinez, Bartolome & de la Cruz, 1988). A unique *Bsp*HI site was created upstream of the ATG start codon in the MCS by amplifying the region between the *Ban*II and *Bal*I sites. The 1.3 kb PCR reaction product was ligated into T-vector (Promega, Madison, WI), transformed into *E. coli* JM110 (Yanisch-Perron, Vieira & Messing, 1985), and the plasmid DNA was isolated and digested with *Ban*II and *Bal*I. The 1.3 kb fragment was purified

Table 1. Bacterial strains and plasmids

	Relevant characteristics	Reference
Strain		
MM2115	Strain MM1925 (*E. coli* K12 wild-type F$^-$/lambda$^-$/IN (*rrnD-rrnE*) with a kan^R insertion into the *mntH* gene	Kehres et al., 2000
JM110	*rpsL (Str^r) thr leu thi-1 lacY galK galT ara tonA tsx dam dcm supE44 D(lac-proAB) [F' traD36 proAB lacI^q ZDM15]*	Yanisch-Perron et al., 1985
Plasmids		
pSU2718	Hybrid pACYC184/pUC18 cloning vector with a chloramphenicol resistance marker and *lac* promoter	Martinez et al., 1988
pDGK201	Plasmid pBluescript-II SK+ containing the *E. coli mntH* gene.	Kehres et al., 2000
pMntH	pSU2718, with the wild-type *mntH* gene under the control of the *lac* promoter	This study
p6HMntH	Same as pMntH except a 6-Histidine tag is located at the amino terminus of MntH	This study

Mutation[a]	Codon change	Protein Expression (% 6Hwild-type)[b]
D34E	GAT to GAG	59.4 ± 16
D34N	GAT to AAC	132.4 ± 40
P35G	CCC to GGC	61.0 ± 18
P35N	CCC to AAC	111.8 ± 19
P35Q	CCC to CAG	128.9 ± 24
G36A	GGT to GCG	141.0 ± 22
G36P	GGT to CCT	110.3 ± 12
N37D	AAC to GAT	114.6 ± 18
N37Q	AAC to CAG	122.0 ± 86
N37S	AAC to TCC	131.2 ± 24
E102Q	GAA to CAG	76.2 ± 11
E102D	GAA to GAC	42.5 ± 13
D109E	GAC to GAG	107.3 ± 10
D109N	GAC to AAT	73.3 ± 13
E112D	GAA to GAC	75.6 ± 23
E112Q	GAA to CAG	91.3 ± 34
G115A	GGT to GCC	91.0 ± 16
G115P	GGT to CCT	77.3 ± 16
E154D	GAG to GAC	142.1 ± 14
E154Q	GAG to CAA	95.1 ± 20
D238E	GAT to GAG	117.5 ± 20
D238N	GAT to AAC	107.6 ± 34

[a]The designated mutations were made using plasmid p6HMntH as the starting material.
[b]Expression levels were measured in strain MM2115 containing the plasmid with the wild-type *6HmntH* gene or a *6HmntH* gene with the designated mutation as described under Materials and Methods.

from a 0.7% agarose gel. The pSU2718 plasmid without the *Bsp*HI site was digested with *Ban*I and *Bal*I and the 1 kb fragment was purified from an agarose gel. The 1.3 kb fragment containing the newly created *Bsp*HI site and the 1 kb vector DNA were ligated to create pSU2718 with a unique *Bsp*HI site in the MCS.

The *mntH* gene was amplified from pDGK201 (Kehres et al., 2000), kindly provided by Dr. Michael Maguire, Case Western Reserve University, using primers that created a unique *Bsp*HI site upstream of the ATG codon and a *Hind*III site immediately after the stop codon. The PCR product and pSU2718 were digested with *Bsp*HI and *Hind*III and ligated together. The resulting plasmid pMntH contains the *mntH* gene under the control of the *lac* promoter.

To create a 6-Histidine-tagged MntH, the *mntH* gene, was amplified from pDGK201 using primers to create a *Bam*HI site prior to the start codon of *mntH* and to add a *Hind*III site just after the stop codon of *mntH*. The 1240 bp PCR product was ligated to T-vector (Promega), transformed into JM110, and the plasmid DNA was isolated and digested with *Bam*HI and *Hind*III. The vector pQE30 (Qiagen, Valencia, CA), which contains a strong promoter and a 6-Histidine tag, was digested with *Bam*HI and *Hind*III. The vector DNA and the 1.2 kb *mntH* fragment were ligated together to create pQE30MntH, which encodes an N-terminal 6-Histidine-tagged MntH (6HMntH).

The *6HmntH* gene fragment of pQE30MntH was amplified using a forward primer to create a unique *Bsp*HI site upstream from the start codon of *6HmntH* and a reverse primer that overlapped a *Hind*III site downstream from the stop codon. The PCR product and pSU2718 were digested with *Bsp*HI and *Hind*III and ligated. The resulting plasmid, p6HMntH, contains the gene for an N-terminal 6-Histidine-tagged MntH under the regulation of the *lac* promoter.

Site-Directed Mutagenesis

Mutants were made using the strategies outlined in the QuikChange mutagenesis kit. The entire *mntH* coding region was sequenced to confirm each mutation.

Mn^{2+} Transport Assays

Cells were grown at 37°C with shaking to mid-log phase in YT media supplemented with 15 μg/mL chloramphenicol and 0.25 mM isopropyl 1-thio-β-D-galactopyranoside. The cells were pelleted by centrifugation at 5000 × *g* for 5 min, and the resulting pellet was washed in 50 mM MES buffer, pH 6.0 and then resuspended in the same buffer at a concentration of approximately 0.5 mg of protein/mL. The cells were then diluted 100-fold in the same buffer and equilibrated at 37°C for 5–10 min before [^{54}Mn]-$MnCl_2$ (5 μCi/mL) was added. Aliquots of 200 μL were removed at appropriate time points, and the cells were captured on 0.45 μm Metricel membranes (Gelman Sciences, Ann Arbor, MI). The cells were then washed with 5–10 mL of ice-cold 50 mM MES buffer by rapid filtration. The filter with the cells was then placed in liquid scintillation fluid and counted using a Beckman LS1801 liquid scintillation counter. Channels 401–945 were used to detect photons derived from γ-radiation of $^{54}Mn^{2+}$.

As a negative control, the strain MM2115/pSU2718, which lacks a functional *mntH* gene, was also subjected to Mn^{2+} transport assays (Martinez et al., 1988; Kehres et al., 2000). The background values from the MM2115/pSU2718 strain were subtracted from the values obtained from the strains carrying the wild-type or mutant *6HmntH* genes.

Membrane Isolation and Western Blot Analysis

Ten milliliters of mid-log cells grown as for transport assays were harvested by centrifugation (5000 × *g*, 10 min). The pellet was resuspended in a cell lysis buffer (50 mM TES, pH 8.0, 100 mM NaCl, 5 mM β-mercaptoethanol, 0.1 mg/mL TPCK, 0.7 μ/mL Pepstatin, and 25 μg/mL PMSF) and quickly frozen in liquid nitrogen and thawed three times. The cell suspension was then sonicated three times for 20 s each. The membrane fraction was harvested by ultracentrifugation (180,000 × *g*, 45 min) and the pellet was resuspended in 200 μL of extraction buffer (50 mM TES, pH 8.0, 100 mM NaCl, 250 mM imidizole, 20% glycerol, 5 mM β-mercaptoethanol, and 0.05% lauryl maltoside). Protein concentrations were determined using a modified Bradford Assay (Bio-Rad). 50 μg samples of each protein were subjected to SDS-polyacrylamide gel electrophoresis. The proteins were electroblotted to nitrocellulose, and Western blot analysis was performed according to Sambrook *et al.* (Sambrook, Fritsch & Maniatas, 1989). The primary polyclonal antibody recognizes the RGS-6H tag (Qiagen). The secondary antibody, goat anti-mouse conjugated to alkaline phosphatase, was purchased from Sigma. The Western blot was then scanned using a Molecular Dynamics laser densitometer and analyzed by comparison to wild-type values for the same preparation and Western blot. As shown in Table 1, the values for each mutant are reported as a percentage of wild-type 6HMntH averaged from three separate preparations.

Kinetic Calculations

For all mutant strains tested, apparent K_m and V_{max} values for $^{54}Mn^{2+}$ transport were determined by observing initial linear rates of transport at five external manganese concentrations (0.1, 0.2, 0.3, 0.5, and 1.0 μM final concentration of Mn^{2+}). For the wild-type strains (pMntH and p6HMntH), the data were linear to 60 seconds. At each concentration, data were collected via rapid filtration at 30-second and 60-second time points in triplicate on three separate days. Thus, the data at each Mn^{2+} concentration for the wild-type strains were based on 18 data points. This strategy was also followed in the analysis of mutant strains except that mutants with lower activity showed linear uptake for longer periods of time. In these cases, the kinetic analysis included data at 3-minute time points in addition to the 30-second and 60-second time points. Since the pH is constant, the transport velocity follows Michaelis-Menten kinetics with respect to $^{54}Mn^{2+}$ concentration (Segel, 1975). Initial estimates of K_m were made using a range of 0.2, 0.5, 1, 2.5 and 5.0 μM final concentration of Mn^{2+} and the concentrations of Mn^{2+} used were readjusted to be 3-fold above and below the K_m for wild-type strains. Results were calculated by an analysis of a plot of *v* vs. [*S*] using the graphic analysis program Excel (Microsoft). Data from three independent runs (each done in triplicate) were averaged to give a value for apparent K_m and V_{max} values, plus or minus SEM.

Results

The Identification of Conserved Residues in MntH

A model for the secondary topology, of *E.coli* MntH has been proposed based on experiments involving Blam and Cat fusions (Courville et al., 2004). To identify conserved residues within this model, we started with the amino-acid sequence of *E. coli* MntH as the query sequence and homologous sequences were identified using the database program BLASTP, version 2.2.1 (Altschul et al., 1997). The top 53 matches that were non-redundant and appeared to be full-length sequences were saved for further analysis. These sequences were subjected to a multiple sequence alignment using the program CLUSTALW (Thompson, Higgins & Gibson, 1994). The multiple sequence alignment was used to identify residues that are conserved among all, or nearly-all, of the 53 sequences. These residues are shown with a bold circle, as they are found in the *E. coli* MntH protein (Figure 1). Six acidic residues were identified that are highly conserved. Of these six residues, four are completely conserved among all 53 sequences. The other two (indicated by bold, shaded circles), at positions 102 and 109 in *E. coli* MntH, are not conserved in two species. Position 102 is changed to an isoleucine in *Clostridium acetylbutylicum* (copy 2), and position 109 is changed to an alanine in *C. acetylbutylicum* (copy 2) and to an asparagine in *Oncorhynchus mykiss* (copy 2).

To compare and slightly refine the model obtained previously by Blam and Cat fusions (Courville et al, 2004), membrane-spanning regions for each of the 53 sequences were also predicted using the program TMHMM (Krogh et al., 2001). These predicted transmembrane regions were overlaid onto the multiple sequence alignment to generate a consensus for the transmembrane regions. This consensus provided the basis for the secondary structural model shown in Fig. 1, which depicts the

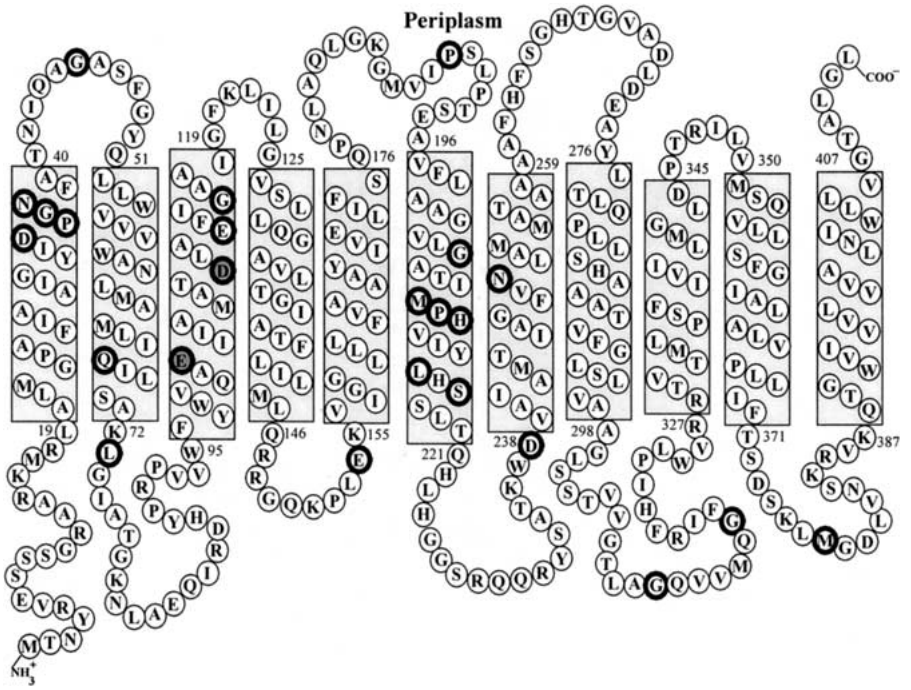

Fig. 1. Secondary topology model of the *E. coli* Nramp homolog, MntH. The amino-acid sequence shown in this figure is *E. coli* MntH. Conserved residues are shown with a darkened circle. With the exception of Glu-102 (98% conserved) and Asp-109 (96% conserved), which are shown as shaded circles, all of these residues are 100% conserved among the 53 members that were analyzed. The secondary structural model was generated in two steps. First, 53 Nramp homologs were aligned using the program CLUSTALW (Thompson et al., 1994). Next, the transmembrane segments in each of the 53 homologs were predicted using the program TMHMM (Krogh et al., 2001). These data were used to produce a consensus for the boundaries of transmembrane regions.

amino-acid sequence of *E. coli* MntH. The model shown in Fig. 1 is only slightly different from the model obtained by Blam and Cat fusions (Courville et al., 2004). Moreover, with regard to most of the residues that are the subject of the current study, there is no disagreement between the two models. In both models, Asp-34, Pro-35, Gly-36, Asn-37, Glu-102, Asp-109, and Glu-112 are found within transmembrane-spanning regions (TMS), and Glu-154 and Asp-238 lie on cytoplasmic loops near the membrane boundary. In our model, Gly-115 is actually within TMS-3, while in their model it is at the TMS-3/aqueous boundary.

Construction of 6HMntH

To begin mutagenesis work on MntH, we first cloned the wild-type *mntH* gene into a vector to create a construct with a 6-Histidine tag at the amino terminus. In the current study, the tag was used to measure the amount of MntH protein using an antibody that recognizes the 6-Histidine tag. Initially, the 6 Histidine-tagged gene was cloned into the vector, pQE30, which has a strong viral promoter. However, expression of the gene caused the cells to grow poorly, so the 6-Histidine construct was cloned next to *lac* promoter within the plasmid, pSU2718 (Martinez et al., 1988). The resulting plasmid is designated p6HMntH.

The wild-type MntH protein and the 6HMntH protein, both under the control of the *lac* promoter, were then compared with regard to their transport properties. As shown in Fig. 2, the two proteins transport $^{54}Mn^{2+}$ to comparable levels. The wild-type protein exhibited an apparent K_m of 0.3 μM and a $V_{max}$of 33.3 nmoles/min mg protein. These values are similar to those reported in other studies (Silver, Johnseine & King, 1970; Kehres et al., 2000). The 6HMntH protein also exhibited a K_m of 0.3 μM, but had a slightly reduced V_{max} of 19.3 nmoles/min mg protein. The reduced V_{max} may be related to a lower level of expression due to the presence of the 6-Histidine tag. However, since an antibody is not available to the wild-type (non-tagged) protein, it was not possible to compare the levels of protein expression. Nevertheless, the moderately high V_{max} value and normal K_m values seen with the 6HMntH protein indicate that the presence of the tag does not significantly perturb structure and function.

Mutagenesis of Conserved Acidic Residues

Because MntH is an H^+/Mn^{2+} symporter, it seemed reasonable to postulate that any or all of the conserved acidic residues might play a role in the binding of H^+ and/or Mn^{2+}. To investigate this possibility, the conserved acidic residues (D34, E102, D109, E112, E154, and D238) were first changed to nonionizable residues of similar size (i.e., aspartic acid to asparagine, and glutamic acid to glutamine). The acidic residues located on transmembrane segments were also substituted with the alternative acidic residue (i.e., aspartic acid for

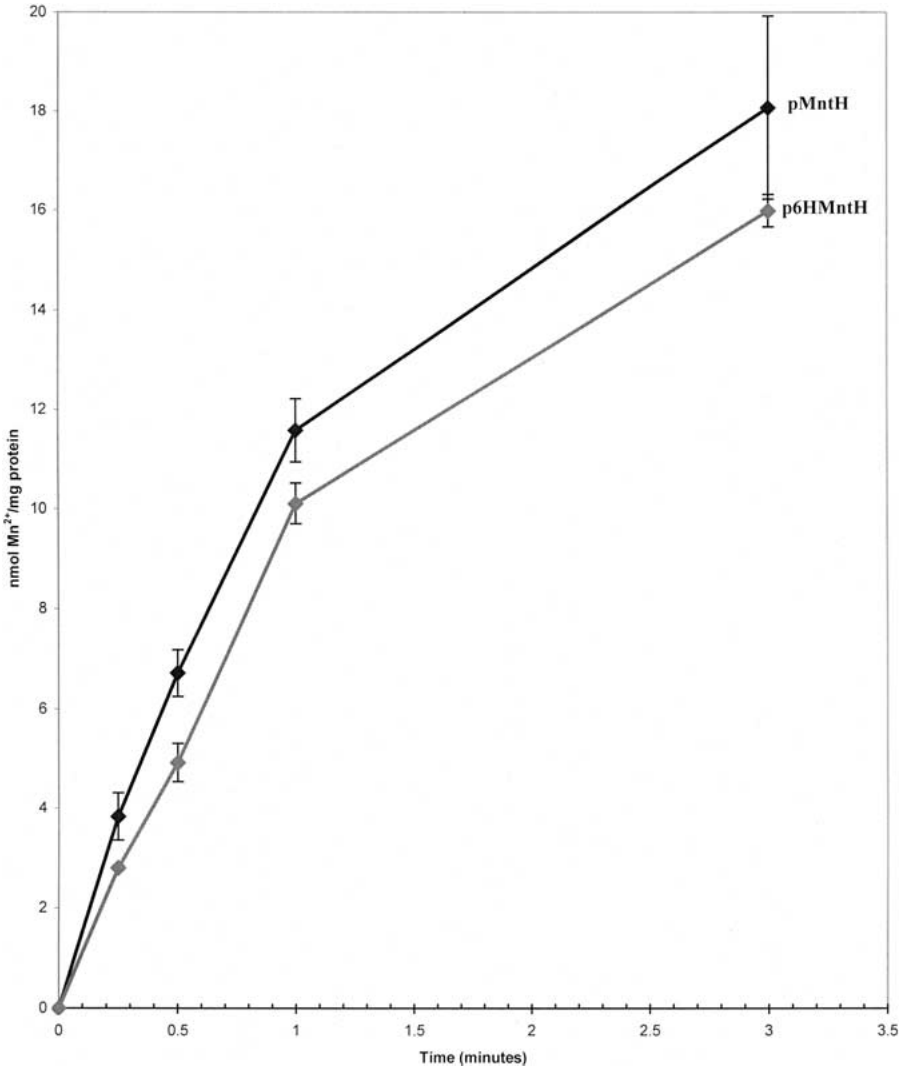

Fig. 2. Transport characterization of wild-type and 6-His-tagged MntH. The transport of $^{54}Mn^{2+}$ was measured at an external concentration of 0.3 μM at 37°C as described under Materials and Methods.

glutamic acid or glutamic acid for aspartic acid). The codon changes are described in Table 1. Also, as seen in this table, the mutants were expressed at moderate to normal levels.

Asp-34 is found within a signature sequence, DPGN, which is conserved in all transporters of the Nramp family (Cellier et al., 1995). Since this sequence contains an acidic residue, it is a reasonable hypothesis that this motif plays an important role that is necessary for the formation of a cation-binding site and/or is required for conformational changes associated with transport. To investigate this possibility, Pro-35, Gly-36, and Asn-37 were also changed to conservative substitutions (*see* Table 1). These mutants were also expressed at moderate to normal levels.

In addition, Gly-115 which is 100% conserved among Nramp family members, was changed to two conservative substitutions. Gly-115 is predicted to lie on the same face of TMS-3 as Asp-109 and Glu-112 (*see* Fig. 1).

Transport Characterization of Wild-Type and Mutant Strains

The mutant strains were initially tested for $^{54}Mn^{2+}$ uptake at 0.3 μM, which is the K_m value for the wild-type strain. Figure 3 shows the mutagenesis results of the conserved acidic residues. The E154Q strain transported Mn^{2+} to levels that were roughly half that of the wild-type strain. In addition, there were a few mutants that transported Mn^{2+} at very low, but detectable rates. These included D109E, D109N, E112D, E112Q, and D238N. The remaining mutants showed transport rates that were indistinguishable from the background transport seen in the knockout strain. Thus, many mutants having conservative substitutions including D34E, D34N, E102D, and E102Q, showed a complete loss of transport activity. With the exception of position 154, these results are consistent with the idea that these residues play an important role in cation binding. Alternatively, these residues could

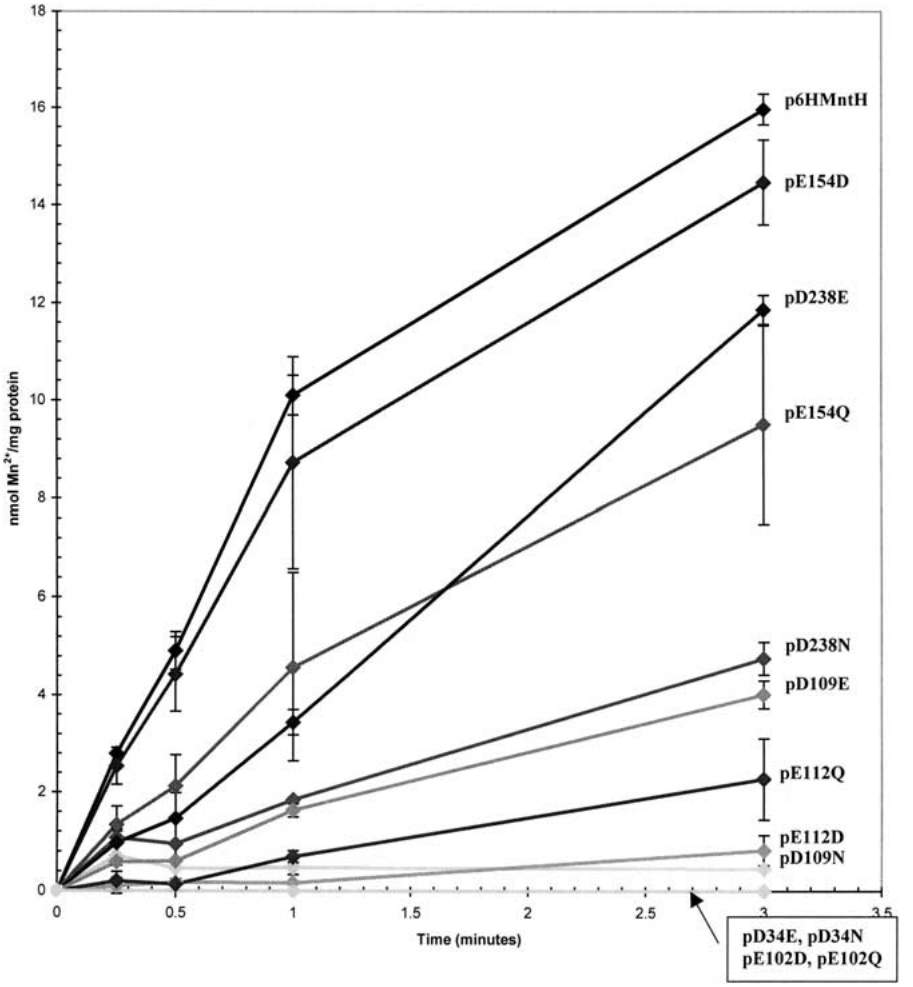

Fig. 3. $^{54}Mn^{2+}$ uptake in 6-His-wild-type and mutant strains that have alterations of conserved acidic residues. The transport of $^{54}Mn^{2+}$ was measured at an external concentration of 0.3 μM at 37°C as described under Materials and Methods.

be important for conformational changes associated with transport, and/or perform a role in maintaining a proper tertiary structure of the protein.

As mentioned, one of the conserved acidic residues, namely Asp-34, is part of the signature motif, DPGN, that is found within the Nramp family. Since Asp-34 appeared critical for transport function, it was of interest to determine if the neutral residues of this motif are also functionally important. Therefore, the other three sites (i.e., Pro-35, Gly-36, and Asn-37) were changed to two or three conservative substitutions and tested for $^{54}Mn^{2+}$ uptake. As shown in Fig. 4, all of the mutants were severely defective in $^{54}Mn^{2+}$ transport. Only the P35G mutant showed any transport that was reliably above background. Similarly, we also investigated the importance of Gly-115, which is a conserved residue in the vicinity of Asp-109 and Glu-112. Two conservative substitutions at Gly-115 showed a complete loss of function. Taken together, these results indicate that conserved neutral residues on TMS-1 and TMS-3 are critically important for MntH function. Since these residues are completely conserved among all Fe^{2+}/Mn^{2+} transporters, a reasonable hypothesis is that they play a key role in the formation of a site that is involved with metal binding.

To further investigate the importance of these residues, the mutants with measurable levels of transport were examined with regard to the kinetics of $^{54}Mn^{2+}$ uptake. These results are presented in Table 2. The E154Q strain had a moderately high V_{max} value and a K_m value that was not significantly different from the wild-type strain. Thus, it appears that a negative charge at position 154 is not critical for cation binding or transport. By comparison, the other mutants tested showed V_{max} values that were less than 15% of the wild-type strain. The D238N mutant had a normal K_m value, whereas the P35G, D109N and E112Q strains had somewhat elevated K_m values. Along these lines, it is interesting to note that Asp-238 is predicted to be located in a hydrophilic loop region that connects TMS-6 and TMS-7, while Pro-35, Asp-109 and Glu-112 are predicted to lie on transmembrane segments both in the model

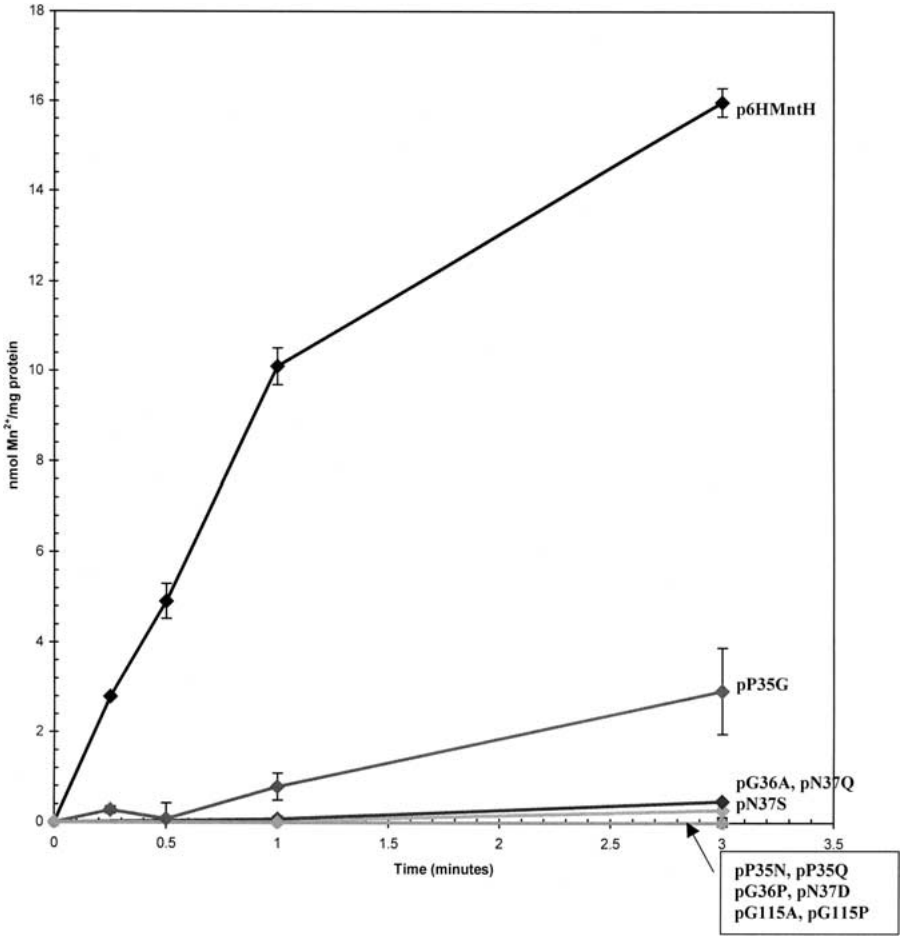

Fig. 4. $^{54}Mn^{2+}$ uptake in 6-His-wild-type and mutant strains that have alterations of conserved neutral residues in TMS-1 and TMS-3. The transport of $^{54}Mn^{2+}$ was measured at an external concentration of 0.3 μM at 37°C as described under Materials and Methods.

Table 2. Kinetic characterization of wild-type and selected mutant strains

Strain	Apparent K_m[a] ± SEM (μM)	Apparent V_{max}[a] ± SEM (nmol mg^{-1} min^{-1})	Adjusted V_{max}[b] (nmol mg^{-1} min^{-1})
6HMntH (wild-type)	0.3 ± 0.1	19.2 ± 7.2	19.2
P35G	0.7 ± 0.1	2.0 ± 0.0	3.3
D109N	0.7 ± 0.2	2.8 ± 1.2	3.8
E112Q	0.9 ± 0.2	2.6 ± 0.9	2.9
E154Q	0.4 ± 0.0	10.0 ± 0.1	10.5
D238N	0.4 ± 0.1	2.6 ± 0.7	2.4

[a]Kinetics measurements were made as described under Materials and Methods.
[b]V_{max} adjusted for differences in protein expression (*see* Table 1).

presented in this study and in another study (Courville et al., 2004).

Discussion

It is interesting to compare our results obtained with *E. coli* MntH with mutants that have been identified in other Nramp homologs. In the rat Nramp2 homolog, Cohen and colleagues found that mutations at Gly-119 (analogous to Gly-36 in MntH) resulted in a complete loss of transport activity, and other mutations in the extracellular loop adjacent to TMS-1 decreased transport activity (Cohen et al., 2003). Surprisingly, one single mutation in the loop (Q126D) caused a complete loss of transport activity, but when combined with another mutation (D124A), transport activity was restored. However, the creation of a triple mutant G119A/D124A/Q126D showed no transport, suggesting an important role for Gly-119 in rat Nramp2. In another study, mutations were made to mouse Nramp2 to neutralize

charge at Asp-86 (MntH Asp-34) and at Glu-154 (MntH Glu-102) (Lam-Yuk-Tseung et al., 2003). In each case, the mutation caused complete loss of iron transport activity, while neutralizing Asp-161 (MntH Asp-109) showed a decrease in transport activity. Interestingly, mutation of the same residues in bacterial and mammalian Nramps appears to yield similar results despite the difference in metal specificity, highlighting the strong functional and structural conservation between family members. It may be the non-conserved residues that create subtle differences in structure around the metal ion binding site that causes a preference for Fe^{2+} by eukaryotic Nramps and a preference for Mn^{2+} in bacteria.

The goal of the current study is the identification of acidic residues that play an important role in the transport mechanism of MntH of *E. coli*. Insights regarding the possible roles of critical residues may be obtained by considering the function of amino acid side chains in other metal-binding proteins whose structures have been determined. Among water-soluble proteins, several are known to bind Fe^{2+} and/or Mn^{2+}, and the amino acid residues that are involved in coordinating the metal ions have been identified for some of these proteins. An interesting example is the Fur repressor protein, which is involved in the regulation of iron uptake genes and the biosynthesis of siderophores in response to iron levels in many species of bacteria. The regulatory metal binding site of the co-repressor Fe^{2+} (and Mn^{2+} or Co^{2+} in vitro) involves at least two histidines and one carboxylate (Adrait et al., 1999).

The manganese-dependent superoxide dismutase (MnSOD), which helps protect cells from oxidative damage by free radicals, consists of two homodimers with each monomer binding one manganese ion. Each manganese ion is coordinated by three histidines, one aspartic-acid residue and one solvent molecule (Edwards et al, 1998). This is also the case for iron-dependent superoxide dismutase (FeSOD) (Lah et al., 1995).

Manganese peroxidases (MnP) are extracellular enzymes excreted by white rot fungi for lignin degradation. The X-ray crystal structure has been solved, showing that a heme propionate group, two water molecules, and three acidic residues of MnP (Glu-35, Glu-39, and Asp-179) interact with Mn^{2+} (Sundaramoorthy et al., 1994).

With these insights, it is interesting to compare the results obtained for MntH in the current study. Among six conserved acidic residues, five are important for function: Asp-34, Glu-102, Asp-109, Glu-112, Asp-238. Of these five, two, Asp-34 and Glu-102 appear to be essential for function, since conservative substitutions at these two sites result in a complete loss of transport function. Likewise, all of the residues within the signature sequence, DPGN, were also mutated in this study. Each residue was changed to several different amino acids, and of ten site-directed mutations made to this motif, only P35G showed any measurable level of $^{54}Mn^{2+}$ uptake with a V_{max} value of approximately 10% of wild-type and a slightly elevated K_m. Prolines and glycines are considered to be helix-breaking residues, with prolines introducing kinks into the helix and glycines contributing to helix flexibility and packing (Ulmschneider & Sansom, 2001). With Asp-34 being an essential negative charge for function, it is possible that Pro-35 and Gly-36 are important for positioning the negative charge in the proper direction for cation binding or for conformational changes that occur during transport. The tolerance for a glycine at position-35 may be explained by its small side-chain volume or added flexibility to the α-helix of TMS 1 that permits transport despite the mutation.

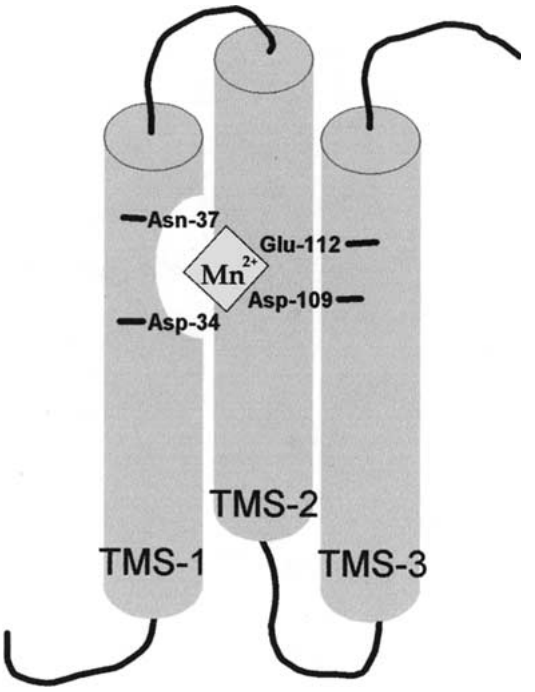

Fig. 5. Hypothetical model for the binding of Mn^{2+} to MntH. In this model, four residues, Asp-34, Asn-37, Asp109, and Glu-112, form a site for the binding of Mn^{2+}. Pro-35, Gly-36, and Gly-115 (*not shown in the figure*) may cause distortions in the helical periodicity of TMS-1 and TMS-3 that help to form this binding pocket. Note: this hypothetical model is based on the effects of mutations on Mn^{2+} transport, and not based on structural or biophysical studies.

Among transporters, the binding and transport of divalent cations has been extensively studied in the Ca^{2+}-ATPase. The results obtained for MntH bear a striking resemblance to the calcium-binding sites in the Ca^{2+}-ATPase. In that transport protein, the Ca^{2+}-binding sites are disrupted by helix breakers, and the residues that form the coordination sites include three carboxylates (Toyoshima et al., 2000; reviewed in MacLennan, Abu-Abed & Kang, 2002).

For example in site I, three carboxylates (Glu-771, Asp-800, and Glu-908), one asparagine (Asn-768), and one threonine (Thr-799) and in site II, the side chain oxygen atoms of Asn-796 and Asp-800 of TMS-6 and Glu-309 of TMS-4 are involved in Ca^{2+} coordination. Another feature of the Ca^{2+}-binding region is a disruption of the α-helical structure in TMS-4 (Pro-312) and in TMS-6 (Gly-801). There is also a high concentration of negatively charged amino-acid residues near TMS-4 at the cytosolic ends of TMS-1 and -3. A very similar arrangement of residues is also found in MntH. In particular, Asp-34, Asn-37, Asp-109, and Glu-112 are found on transmembrane segments 1 and 3 near the periplasmic side (*see* Fig. 1). Furthermore, these residues are in the vicinity of helix breakers (Pro-35, Gly-36, and Gly-115) that are critical for function. Based on these analogies, Fig. 5 depicts a hypothetical binding pocket for the Mn^{2+} ion, when it is bound to MntH. The model does not include Glu-102 or Asp-238 because these residues are located near the cytoplasmic side of TMS-3 and TMS-7, respectively. Even so, Glu-102 and/or Asp-238 could play a role in the release of Mn^{2+} from the binding pocket and its transport into the cytoplasm. Alternatively, they could play a role in maintaining secondary structure.

Finally, it is important to mention that since MntH is postulated to be an H^+/Mn^{2+} symporter, acidic residues could also play a role in H^+ recognition and transport. Alternatively, the actual transported species may be H_3O^+, which also could be coordinated by acidic residues. A detailed proton translocation mechanism has been largely elucidated for bacteriorhodopsin, a membrane-spanning ion pump, which converts light energy into an electrochemical gradient by pumping protons out of the cytoplasm. Asp-85 serves as the initial proton acceptor until the late stages of the photocycle when the proton is released through an H-bonded network of residues (Arg-82, Glu-194, and Glu-204) to the extracellular medium. Finally, Asp-96 is involved in reprotonation for the next photocycle (Lanyi & Schobert, 2002; Luecke et al., 2000).

In the current study involving MntH, the mutants had such low activity that it was not possible to measure H^+ transport directly. However, the lowering of the assay pH to 5.0 or 5.5 was unable to rescue transport activity of D34E, D34N, E102D, and E102Q or any of the other mutations made to the DPGN motif (*data not shown*), making it less likely that these residues are involved in proton transport. Lowering pH has been shown in previous studies to restore transport activity to double-histidine mutants of Nramp2 (Lam-Yuk-Tseung et al., 2003). The authors hypothesized that two histidine residues in TMS-6 may be important for a proton relay system but not for metal binding. Mutation of these two residues to cysteines (which can also form a metal-binding site) showed no metal transport, but changing the pH of the assay could restore metal transport in the double cysteine mutant (Lam-Yuk-Tseung et al., 2003).

As the first step in structure/function analysis of MntH, this study determined the importance of highly conserved residues in the Nramp family that could be potential metal ion or proton binding sites. In this study, the results are striking in that residues clustered on TMS-1 and TMS-3 appear essential for transport. These include three negatively charged residues (Asp-34, Glu-102, and Asp-109) and four other nearby residues (Pro-35, Gly-36, Asn-37, and Gly-115), all of which are 100% conserved in the Nramp family. Additional nearby residues that are not conserved may be important in providing differences in metal-ion specificity among the family members. Further work will be needed to determine the specific role of each of these residues to elucidate the mechanism by which Nramp family members co-transport divalent metal ions and H^+ or H_3O^+.

This work was supported by a seed grant from the Biotechnology Institute of the University of Minnesota. Heather Haemig has been supported by the NIH Biotechnology Training Grant (IT32-GM08347). We are particularly grateful to Dr. Michael Maguire (CWRU) and Dr. David Kehres (CWRU) for providing us with bacterial strain (MM2115), plasmid (pDGK201), and numerous helpful discussions. We also thank Teresa DelaMora for help with the making of the P35G, G36A, and N37Q mutants.

References

Adrait, A., Jacquamet, L., Le Pape, L., Gonzalez de Peredo, A., Aberdam, D., Hazemann, J.L., Latour, J.M., Michaud-Soret, I. 1999. Spectroscopic and saturation magnetization properties of the manganese- and cobalt-substituted Fur (ferric uptake regulation) protein from Escherichia coli. *Biochemistry* **38:**6248–6260

Altschul, S.F., Madden, T.L., Schaffer, A.A., Zhang, J., Zhang, Z., Miller, W., Lipman, D.J. 1997. Gapped BLAST and PSI-BLAST: a new generation of protein database search programs. *Nucleic Acids Res.* **25:**3389–33402

Andrews, S.C., Robinson, A.K., Rodriguez-Quinones, F. 2003. Bacterial iron homeostasis. *FEMS Microbiol* **Rev.27:**215–37

Braun, V., Braun, M. 2002. Iron transport and signaling in *Escherichia coli. FEBS Lett.* **529:**78–85

Cellier, M., Prive, G., Belouchi, A., Kwan, T., Rodrigues, V., Chia, W., Gros, P. 1995. Nramp defines a family of membrane proteins. *Proc. Natl. Acad. Sci. USA* **92:**10089–10093

Cellier, M.F., Bergevin, I., Boyer, E., Richer, E. 2001. Polyphyletic origins of bacterial Nramp transporters. *Trends Genet* **17:**365–370

Cohen, A., Nevo, Y., Nelson, N. 2003. The first external loop of the metal ion transporter DCT1 is involved in metal ion binding and specificity. *Proc. Natl. Acad. Sci. USA* **100:**10694–10699

Courville, P., Chaloupka, R., Veyrier, F., Cellier, M.F. 2004. Determination of transmembrane topology of the *Escherichia coli* natural resistance-associated macrophage protein (Nramp) ortholog. *J. Biol. Chem.* **279:**3318–3326

Crowley, J., Traynor, D., Weatherburn, D. 2000. Enzymes and Proteins containing manganese: an overview. *Met. Ions Biol. Syst.* **37:**211–257

Curie, C., Alonso, J.M., Le Jean, M., Ecker, J.R., Briat, J.F. 2000. Involvement of NRAMP1 from *Arabidopsis thaliana* in iron transport. *Biochem. J. 347 Pt* **3:**749–755

D'Souza, J., Cheah, P.Y., Gros, P., Chia, W., Rodrigues, V. 1999. Functional complementation of the malvolio mutation in the taste pathway of *Drosophila melanogaster* by the human natural resistance-associated macrophage protein 1 (Nramp-1). *J. Exp. Biol.* **202:**1909–1915

Edwards, R., Baker, H., Whittaker, M., Whittaker, J., Jameson, G., Baker, E. 1998. Crystal structure of *Escherichia coli* manganese superoxide dismutase at 2.1-A resolution. *J. Biol. Inorg. Chem.* **3:**161–171

Fleming, M.D., Trenor, C.C. 3rd, Su, M.A., Foernzler, D., Beier, D.R., Dietrich, W.F., Andrews, N.C. 1997. Microcytic anaemia mice have a mutation in Nramp2, a candidate iron transporter gene. *Nat. Genet.* **l6:**383–386

Gruenheid, S., Cellier, M., Vidal, S., Gros, P. 1995. Identification and characterization of a second mouse Nramp gene. *Genomics* **25:**514–525

Gunshin, H., Mackenzie, B., Berger, U.V., Gunshin, Y., Romero, M.F., Boron, W.F., Nussberger, S., Gollan, J.L., Hediger, M.A. 1997. Cloning and characterization of a mammalian proton-coupled metal-ion transporter. *Nature* **388:**482–488

Kehres, D.G., Zaharik, M.L., Finlay, B.B., Maguire, M.E. 2000. The NRAMP proteins of *Salmonella typhimurium* and *Escherichia coli* are selective manganese transporters involved in the response to reactive oxygen. *Mol. Microbiol.* **36:**1085–1100

Kraft, R., Tardiff, J., Krauter, K.S., Leinwand, L.A. 1988. Using mini-prep plasmid DNA for sequencing double stranded templates with Sequenase. *Biotechniques* **6:**544–547

Krogh, A., Larsson, B., von Heijne, G., Sonnhammer, E.L. 2001. Predicting transmembrane protein topology with a hidden Markov model: application to complete genomes. *J. Mol. Biol.* **305:**567–580

Lah, M.S., Dixon, M.M., Pattridge, K.A., Stallings, W.C., Fee, J.A., Ludwig, M.L. 1995. Structure-function in Escherichia coli iron superoxide dismutase: comparisons with the manganese enzyme from *Thermus thermophilus*. *Biochemistry* **34:**1646–1660

Lam-Yuk-Tseung, S., Govoni, G., Forbes, J., Gros, P. 2003. Iron transport by Nramp2/DMT1: pH regulation of transport by 2 histidines in transmembrane domain 6. *Blood* **101:**3699–3707

Lanyi, J., Schobert, B. 2002. Crystallographic structure of the retinal and the protein after deprotonation of the Schiff base: the switch in the bacteriorhodopsin photocycle. *J. Mol. Biol.* **321:**727–737

Luecke, H., Schobert, B., Cartailler, J.P., Richter, H.T., Rosengarth, A., Needleman, R., Lanyi, J.K. 2000. Coupling photoisomerization of retinal to directional transport in bacteriorhodopsin. *J. Mol. Biol.* **300:**1237–1255

MacLennan, D.H., Abu-Abed, M., Kang, C. 2002. Structure-function relationships in Ca(2+) cycling proteins. *J. Mol. Cell. Cardiol.* **34:**897–918

Makui, H., Roig, E., Cole, S.T., Helmann, J.D., Gros, P., Cellier, M.F. 2000. Identification of the *Escherichia coli* K-12 Nramp orthologue (MntH) as a selective divalent metal ion transporter. *Mol. Microbiol.* **35:**1065–1078

Martinez, E., Bartolome, B., de la Cruz, F. 1988. pACYC184-derived cloning vectors containing the multiple cloning site and lacZ alpha reporter gene of pUC8/9 and pUC18/19 plasmids. *Gene* **68:**159–162

Pinner, E., Gruenheid, S., Raymond, M., Gros, P. 1997. Functional complementation of the yeast divalent cation transporter family SMF by NRAMP2, a member of the mammalian natural resistance- associated macrophage protein family. *J. Biol. Chem.* **272:**28933–28938

Reeve, I., Hummel, D., Nelson, N., Voss, J., Hummell, D. 2002. Overexpression, purification, and site-directed spin labeling of the Nramp metal transporter from *Mycobacterium leprae*. *Proc. Natl. Acad. Sci. USA* **99:**8608–8613

Richer, E., Courville, P., Bergevin, I., Cellier, M.F. 2003. Horizontal gene transfer of "prototype" Nramp in bacteria. *J. Mol. Evol.* **57:**363–76

Sambrook, J., Fritsch, E.F., Maniatas, T. 1989. Molecular Cloning: A Laboratory Manual. Cold Spring Harbor Laboratory, Cold Spring Harbor, NY,

Segel, I. 1975. Enzyme Kinetics. Wiley and Interscience, New York,

Silver, S., Johnseine, P., King, K. 1970. *J. Bacteriology* **104:**1299–1306

Su, M.A., Trenor, C.C., Fleming, J.C., Fleming, M.D., Andrews, N.C. 1998. The G185R mutation disrupts function of the iron transporter Nramp2. *Blood* **92:**2157–2163

Sundaramoorthy, M., Kishi, K., Gold, M.H., Poulos, T.L. 1994. The crystal structure of manganese peroxidase from *Phanerochaete chrysosporium* at 2.06-A resolution. *J. Biol. Chem.* **269:**32759–32767

Thomine, S., Wang, R., Ward, J.M., Crawford, N.M., Schroeder, J.I. 2000. Cadmium and iron transport by members of a plant metal transporter family in Arabidopsis with homology to Nramp genes. *Proc. Natl. Acad. Sci. USA* **97:**4991–4996

Thompson, J.D., Higgins, D.G., Gibson, T.J. 1994. CLUSTAL W: improving the sensitivity of progressive multiple sequence alignment through sequence weighting, position-specific gap penalties and weight matrix choice. *Nucleic Acids Res.* **22:**4673–4680

Toyoshima, C., Nakasako, M., Nomura, H., Ogawa, H. 2000. Crystal structure of the calcium pump of sarcoplasmic reticulum at 2.6 A resolution. *Nature* **405:**647–655

Ulmschneider, M.B., Sansom, M.S. 2001. Amino acid distributions in integral membrane protein structures. *Biochim. Biophys. Acta* **1512:**1–14

Winkelmann, G. 2002. Microbial siderophore-mediated transport. *Biochem. Soc. Trans.* **30:**691–696

Yanisch-Perron, C., Vieira, J., Messing, J. 1985. Improved M13 phage cloning vectors and host strains: nucleotide sequences of the M13mp18 and pUC19 vectors. *Gene* **33:**103–119